Preparation and Characterization of LLDPE/LLDPE-*g*-Polyether Pentaerythriol Mono-Maleate Blends Film

WENFEI LI[1,*], ZHANHAI YAO[2] and SHUMEI LIU[1]

[1]College of Chemistry and Environmental Engineering, Changchun University of Science and Technology, Changchun 130022, P.R. China
[2]State Key Laboratory of Polymer Physics and Chemistry, Changchun Institute of Applied Chemistry, Chinese Academy of Sciences, Changchun 130022, P.R. China

*Corresponding author: E-mail: liwenfei1130@126.com

Blends of linear low density polyethylene (LLDPE) and linear low density polyethylene-grafted-polyether pentaerythriol mono-maleate (LLDPE-*g*-PPMM) were prepared by melt mixing. The surface of film with different contents LLDPE-*g*-PPMM was characterized through contact angle measurement, FT-IR spectroscopy and X-ray photoelectron spectroscopy (XPS). The contact angles of water and glycerol on film surface of LLDPE/LLDPE-*g*-PPMM blends decrease with increase of LLDPE-*g*-PPMM. From FT-IR spectra of the blends, the carbonyl peak strength on the film surface was calculated. It was found that larger the carbonyl peak strength, the lower the value contact angle for LLDPE/LLDPE-*g*-PPMM blends.

Keywords: LLDPE-*g*-PPMM, Film, Contact angle.

INTRODUCTION

In both composite polymer structures and polymer blends the compatibilization of the polymer/polymer interfaces is of critical importance. It is well known that most of the polymer pairs are immiscible and do not have strong enough interactions[1,2]. However, several compatibilizations strategies have emerged to resolve the poor adhesion between polymer pairs[3,4]. Func-tonalization of polyolefines through graft copolymerization of unsaturated monomer containing polar groups has received considerable attention in recent years[5,6], especially in the modification of some of the properties, like adhesion, dyeability and wettability.

Polyethylene is one of the most widely used polyolefins. Since it does not include any polar group in its backbone, their poor reactivity, dyeability and hygroscophilicity limit their potential. Many modification methods have been used to improve the wettability of polyethylene, such as plasma tretment[7], living radical grafting polymerization[8], chemical graft polymerization[9], photo[10] and high-energy radiation[11] induced grafting, *etc*. The modification of polyolefins with polar monomers by reactive extrusion has received much attention in the past several decades. By this method, some properties of polyolefins such as polarity, wettability, adhesion with metal, glass or ceramic and compatibility with polyamides, polyesters, *etc*. could be greatly improved[12-14].

Blends of modified polymer change the polar groups on the surface of polymer. Contact angle measurement of a solid and liquid interface is a widely used method for determination of the surface energy of solid polymer. This technique is an excellent method for characterizing the surface, giving information on the wetting behaviour of a liquid on a solid surface. FT-IR is a well-accepted method for identification and quantification of the polar group that are present in a polymer surface.

In this work, the surface of blends of linear low density polyethylene (LLDPE) and linear low density polyethylene-grafted-polyether pentaerythriol mono-maleate (LLDPE-*g*-PPMM) were characterized by contact angle measurements, XPS, as well as FT-IR from which the carbonyl peak strength on the polymer surface has been obtained.

EXPERIMENTAL

The materials used in this work were a linear low density polyethylene (LLDPE) and linear low density polyethylene-grafted-polyether pentaerythriol mono-maleate (LLDPE-*g*-PPMM). The LLDPE was purchased from China Petrol Daqing Petrochemical Co. (China), its trade name is DFDA7042. The LLDPE-*g*-PPMM was prepared in our laboratory. The main characteristics of LLDPE and LLDPE-*g*-PPMM are reported in Table-1. The LLDPE-*g*-PPMM contains 1.57 % polyether pentaerythriol mono-maleate (PPMM). Deionized water with a surface tension of 72.75 mN/m was used for the contact

angle measurements. Glycerol of analytical grade was purchased from Beijing Chemical Factory (China). Xylene was used for extraction experiments.

Preparation of blends: Blends of LLDPE with overall contents of 0, 20, 40, 60, 80 and 100 wt. % of LLDPE-*g*-PPMM were prepared by melt mixing in a SHJ-30 co-rotating twin screw extruder. The diameter of the screws was 30 mm and the ratio of length to diameter (L/D) was 44. The processing temperature was set at 200 °C and the screw run speed was 100 rpm.

Preparation of films: Cast films of the LLDPE/LLDPE-*g*-PPMM blends were obtained using xylene at 120 °C and cast them on a glass plate. All the LLDPE/LLDPE-*g*-PPMM films were dried under a reduced pressure, placed between two leaves of filter paper and stored in a desiccator kept at 25 °C and 60 % relative humidity.

Contact angle measurements: Contact angle measurement was made with a JY-82 contact angle goniometer (Chengde Test Machine Co., Ltd. China) at ambient humidity and temperature. The polar liquids droplets ranging from 0.5-1 mm in diameter were prepared with a microsyringe, they were placed on the surface of LLDPE/LLDPE-*g*-PPMM films. The contact angles of water and glycerol on surface of LLDPE-*g*-PPMM films were measured by using a home made apparatus. Each contact angle was the mean of at least eight measurements.

Surface structure: FT-IR spectra were obtained by means of a Bruker Vertex 70 Spectrometer on compression molded films of the LLDPE/LLDPE-*g*-PPMM blends. The films were pressed at 180 °C. Each spectrum was recorded from 4000 to 400 cm^{-1} with a total of 32 scans.

X-Ray photoelectron spectroscopy (XPS) analysis: The chemical composition of film surfaces was analyzed by XPS with a VG ESCALAB MKII instrument with an MgK$_\alpha$ X-ray source (1253.6).

RESULTS AND DISCUSSION

Contact angle of measurement: The contact angles of water and glycerol on surface of LLDPE/LLDPE-*g*-PPMM films are listed in Table-2. As can be seen, the contact angle of the LLDPE/LLDPE-*g*-PPMM blends decrease with increase of the LLDPE-*g*-PPMM content. The contact angle of water

and glycerol show no significant changes when LLDPE-*g*-PPMM content lower 20 %. On the other hand, for LLDPE-*g*-PPMM content higher 40 %, the contact angle shows a notable reduction with increase of LLDPE-*g*-PPMM. The contact angle is very sensitive to the chemical and structural changes that occur on polymer surfaces, since the liquid makes contact with the outermost molecular layer of the surface.

It is well known that the contact angle between liquid and solid is expressed by Young's equation

$$\gamma_L \cos\theta = \gamma_S - \gamma_{SL} - \pi_e \tag{1}$$

where γ_S and γ_L are the surface tension of solid and liquid, respectively and γ_{SL} is the interfacial tension between solid and liquid. The spreading pressure π_e can be neglected because $\pi_e \ll \gamma_L$. Using eqn. 1 and Dupre's equation

$$W_A = \gamma_S + \gamma_L - \gamma_{SL} \tag{2}$$

The equation of Young-Dupre equation is expressed as:

$$W_A = \gamma_L (1 + \cos\theta) \tag{3}$$

Combining the harmonic-mean equation[15] with Young-Dupre equation gives

$$W_A = 4[\gamma_S^d \gamma_L^d / (\gamma_S^d + \gamma_L^d) + \gamma_S^p \gamma_L^p / (\gamma_S^p + \gamma_L^p)] \tag{4}$$

whereas combining the geometric-mean equation with Young-Dupre equation gives

$$W_A = 2[(\gamma_S^p \gamma_L^p)^{1/2} + (\gamma_S^d \gamma_L^d)^{1/2}] \tag{5}$$

where W_A is the work of adhesion, θ is the contact angle, γ_S^d and γ_L^d are dispersion components of surface free energy for the solid and liquid, respectively. The γ_S^p and γ_L^p are polar component of surface free energy for the solid and liquid, respectively.

The γ_L^d and γ_L^p for water and glycerol are reported in Table-3. The γ_S^d and γ_S^p could be calculated by solving eqn. 3 and 5 for water and glycerol. The values of γ_S^d and γ_S^p are shown in Table-4. It can be observed that the total surface energy increase with increase of LLDPE-*g*-PPMM content. The increased surface energy of the LLDPE/LLDPE-*g*-PPMM blend comes mostly from the polar component when the LLDPE-*g*-PPMM content increases. This indicates that, due to the presence of polar groups

TABLE-3			
γ_L^d AND γ_L^p FOR WATER AND GLYCEROL			
Liquids	γ_L^d (mJ/m²)	γ_L^p (mJ/m²)	γ_L (mJ/m²)
Water	22.08	50.67	72.75
Glycerol	40.52	22.85	63.37

TABLE-2				
CONTACT ANGLES (θ) AND WORK OF ADHESION (W_A) FOR FILMS OF LLDPE/LLDPE-*g*-PPMM BLENDS				
LLDPE/LLDPE-*g*-PPMM wt/wt	θ of Water (°)	W_A of water (mN/m)	θ of Glycerol (degree)	W_A of Glyceyol (mN/m)
100/0	89	74.02	72	82.95
80/20	78	87.87	62	93.12
60/40	65	103.49	52	102.38
40/60	39	129.29	35	115.27
20/80	28	136.98	25	120.80
0/100	13	143.64	11	125.57

on the surface of LLDPE/LLDPE-*g*-PPMM, the surface energies of blends are expected to increase as a function of LLDPE-*g*-PPMM content. The results of work of adhesion calculated according to eqn. 3 are listed in Table-2. Because the contact angle decreases with increase of LLDPE-*g*-PPMM content, the work of adhesion increases.

TABLE-4
SURFACE ENERGY FOR THE FILMS OF
LLDPE/LLDPE-*g*-PPMM BLENDS

LLDPE/LLDPE-*g*-PPMM (wt/wt)	γ_s^d (mJ/m^2)	γ_s^p (mJ/m^2)	Total surface energy (mJ/m^2)
100/0	26.81	3.17	29.98
80/20	28.30	7.13	35.43
60/40	26.31	15.13	41.44
40/60	19.62	38.07	57.69
20/80	20.16	44.49	64.65
0/100	20.43	50.69	71.12

FT-IR analysis: The FT-IR spectra of the pure LLDPE and LLDPE/LLDPE-*g*-PPMM are shown in Fig. 1. It is clearly seen that for LLDPE/LLDPE-*g*-PPMM blends appear absorption peaks at 1722 cm^{-1}, which are attributed to contributions of carbonyl of LLDPE-*g*-PPMM. But spectra of LLDPE film has not absorption peak at 1722 cm^{-1}.
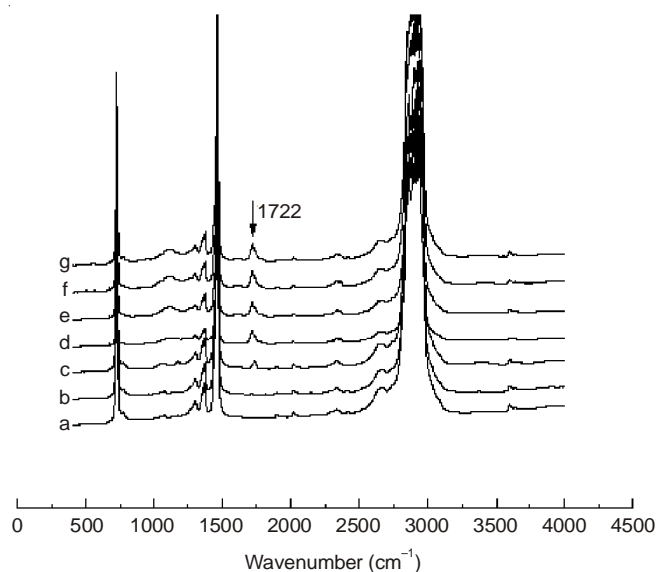

Fig. 1. FT-IR spectra of film surfaces of LLDPE/LLDPE-*g*-PPMM with different LLDPE-*g*-PPMM content; a: LLDPE/LLDPE-*g*-PPMM 100/0, b: LLDPE/LLDPE-*g*-PPMM 90/10, c: LLDPE/LLDPE-*g*-PPMM 80/20, d: LLDPE/LLDPE-*g*-PPMM 60/40, e: LLDPE/LLDPE-*g*-PPMM 40/60, f: LLDPE/LLDPE-*g*-PPMM 20/80, g: LLDPE/LLDPE-*g*-PPMM 0/100

The carbonyl peak strength of LLDPE/LLDPE-*g*-PPMM are shown in Table-5. Defining carbonyl peak strength as the ratio between the absorption peak at 1722 and 1378 cm^{-1} height, it was observed that the carbonyl peak strength increased with LLDPE-*g*-PPMM content. This increase in carbonyl peak strength indicated that the film surface of LLDPE/LLDPE-*g*-PPMM contains more amount carbonyl polar groups. The higher values of carbonyl peak strength, the lowering of the contact angle is. Higher carbonyl peak strength means more carbonyl groups are present on the surface and the surface energy of LLDPE/LLDPE-*g*-PPMM would be improved.

XPS analysis: XPS spectra for LLDPE and LLDPE/LLDPE-*g*-PPMM are shown in Figs. 2 and 3. The C 1s core-level spectrum for pure LLDPE is shown in Fig. 2. The peak
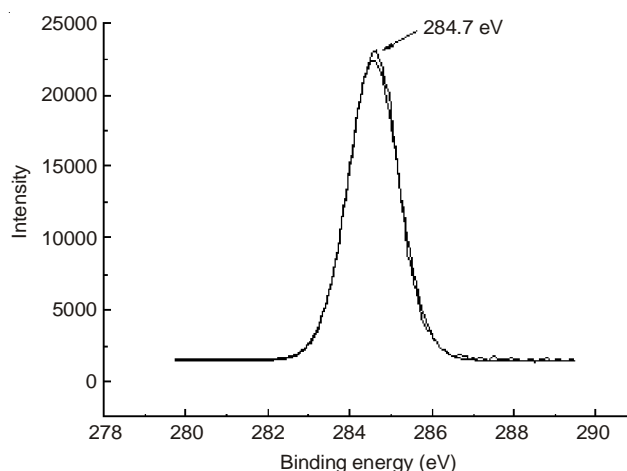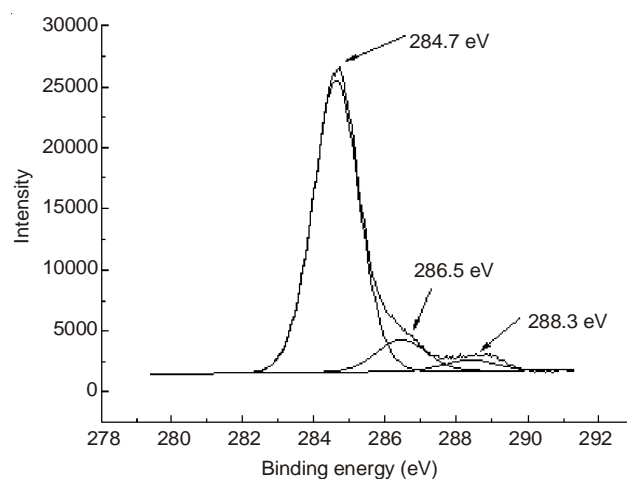

Fig. 2. XPS C 1s spectrum for pure LLDPE

Fig. 3. XPS C 1s spectrum for LLDPE/LLDPE-*g*-PPMM

TABLE-5
CARBONYL PEAK STRENGTH (C$_S$), PEAK HEIGHT (P$_h$) AND CONTACT ANGLE (θ)
OF FILMS OF LLDPE/LLDPE-*g*-PPMM WITH DIFFERENT LLDPE-*g*-PPMM CONTENT

LLDPE/LLDPE-*g*-PPMM (wt/wt)	P$_h$ of 1712 (cm^{-1})	P$_h$ of 1378 (cm^{-1})	C$_S$	θ of water (°)
100/0	0	5.7862	0	89
80/20	1.9985	4.4887	0.45	78
60/40	2.1026	2.5073	0.84	65
40/60	3.0625	3.4987	0.87	39
20/80	4.0016	4.4982	0.89	28
0/100	4.0324	4.0115	1.01	13

is narrow and symmetric for organic carbon species with binding energy at 284.7 eV. In Fig. 3, the spectrum for LLDPE/LLDPE-*g*-PPMM contains two additional peaks with binding energy at 286.5 eV for a carbon single bond (C-O) to oxygen species and at approximately 288.3 eV for C=O species, which are attributed to contributions of PPMM in LLDPE/LLDPE-*g*-PPMM film surface.

Conclusion

The contact angle of water and glycerol on surface of LLDPE/LLDPE-*g*-PPMM blends decrease with the LLDPE-*g*-PPMM content. The total surface energy and work of adhesion of films of LLDPE/LLDPE-*g*-PPMM blends increase with increase of LLDPE-*g*-PPMM content. Carbonyl polar groups on the surface of LLDPE/LLDPE-*g*-PPMM films increase with increase of LLDPE-*g*-PPMM content in LLDPE/LLDPE-*g*-PPMM blends.

REFERENCES

1. O.M. Istrate, M.A. Gunning, C.L. Higginbotham and B.G. Chen, *J. Polym. Sci., B, Polym. Phys*., **50**, 431 (2012).
2. J.H. Yang, J.L. White and Q.B. Jiang, *Polym. Eng. Sci*., **50**, 1969 (2010).
3. M. Entezam, H.A. Khonakdar, A.K. Yousefi, S.H. Jafari, U. Wagenknecht, G. Heinrich and B. Kretzschmar, *Macromol. Mater. Eng*., **297**, 312 (2012).
4. H.S. Lee and J.D. Kim, *Polym. Compos*., **33**, 1154 (2012).
5. I. Fortelny, L.I. Minkova, L. Kotek, M. Lapcikova and D. Michalkova, *Polym. Eng. Sci*., **52**, 191 (2012).
6. P. Ma, D.G. Hristova-Bogaerds, P.J. Lemstra, Y. Zhang and S.F. Wang, *Macromol. Mater. Eng*., **297**, 402 (2012).
7. N. John and V. Singh, *Int. J. Polym. Mater*., **60**, 255 (2011).
8. P.R. Yu, G.L. Wu, J.Y. Peng, S.A. Hu, Y.Q. Xiong and W.J. Xu, *J. Macromol. Sci*., **48**, 416 (2011).
9. M. Hemmati, A. Narimani, H. Shariatpanahi, A. Fereidoon and M.G. Ahangari, *Int. J. Polym. Mater*., **60**, 384 (2011).
10. A. Khot, A. Bailey, T. Debies and G.A. Takacs, *J. Adhes. Sci. Technol*., **26**, 2627 (2012).
11. X.M. Tan and Y.S. Xu, *Radiation Effects Defects Solids*, **163**, 107 (2008).
12. A. Farzadfar and S.N. Khorasani, *Polymer-Plastics Technol. Eng*., **51**, 1424 (2012).
13. R. Doufnoune, N. Haddaoui and F. Riahi, *Int. J. Polym. Mater*., **57**, 690 (2008).
14. H.J. Shao, S.H. Qin, J. Yu and J.B. Guo, *Polymer-Plastics Technol. Eng*., **51**, 28 (2012).
15. S. Wu, Polymer Interface and Adhesion, New York, pp. 152-153 (1982).